AN APPROACH TO PREDICT THE GALVANIC CORROSION BEHAVIOR OF IDENTICAL COUPLE ELECTRODES: AZ91D MAGNESIUM ALLOY AND HVOF SPRAYED TITANIA COATED AZ91D MAGNESIUM ALLOY

[1] Daniel C. Ribu*, [2]R.Rajesh and [3] D.Thirumalaikumarasamy

[1]Daniel C. Ribu (**Corresponding Author**)*
Assistant Professor,
Department of Mechanical Engineering,
Lourdes Matha College of Science and Technology,
Thiruvananthapuram – 608 002,
Kerala,
INDIA.
Email: ribucdaniel@gmail.com
Tel: +91-09995453358 (Mobile)

[2]R.Rajesh
Professor and Principal
Department of Mechanical Engineering,
Rohini College of Engineering & Technology,
Anjugramam– 629401,
Tamil Nadu,
INDIA.
Email: rajesh1576@yahoo.co.in
Tel: +91-09894434131
Fax: +91-4652-266605

[3]D.Thirumalaikumarasamy
Assistant Professor,
Department of Mechanical Engineering,
Government College of Engineering,
Bargur– 635104,
Krishnagiri.
Tamil Nadu,
INDIA.
Email: tkumarasamy412@gmail.com
Tel: +91-09894319865(Mobile)
Fax: +91-4144-238080/238275

Abstract

The corrosion of AZ91D magnesium alloy has received extensive attention owing to the continuous expansion of its application field in recent years. However, the corrosion of AZ91D magnesium alloy in sodium chloride environment is relatively few. Corrosion behaviour of the AZ91D magnesium alloy was evaluated by conducting immersion corrosion test in NaCl solution at different chloride ion concentrations, pH value and immersion time. An attempt was also made to develop an empirical relationship to predict the corrosion rate of AZ91D magnesium alloy. Three factors, five level, central composite rotatable design matrix was used to minimize the number of experimental conditions. Response surface methodology was used to develop the relationship. The developed relationship can be effectively used to predict the corrosion rate of AZ91D magnesium alloy at 95 % confidence level. Results showed that pH value greatly influence the galvanic corrosion behavior of HVOF sprayed TiO_2 coatings followed by chloride ion concentrations and immersion time.

Keywords: AZ91D magnesium alloy; Chloride ion concentration; Response surface methodology; Corrosion rate

Abbreviations:

RSM: Response surface methodology

CR: Corrosion rate

XRD: X-ray diffraction

1. Introduction

Magnesium (Mg) alloys offer the advantages of high specific strength/stiffness, better shock absorption, and easy processing, attracting increasing interest for use in the automotive, aerospace, electronics, and transportation industries. However, their wider

industrial applications are severely limited by their poor corrosion and wear resistance performance. Surface coating is an effective method to improve the comprehensive performance of Mg alloys. The common surface treatment methods used on Mg alloys mainly include vapor deposition, anodic oxidation, micro arc oxidation, electro deposition, chemical conversion coatings, and thermal spraying [1-6].

When two dissimilar metals in electrical contact are exposed to a common electrolyte, one of the metals can undergo increased corrosion, while the other can show decreased corrosion. This type of accelerated corrosion is referred to as galvanic corrosion. Because galvanic corrosion can occur at a high rate, it is important that a means be available to alert the user of the product or equipment that involves the use of dissimilar metal combinations in an electrolyte of the possible effects of galvanic corrosion. The galvanic corrosion test was carried out as per ASTM G 71 (2004) [7]. This standard guide covers the development of a galvanic series, and its subsequent use as a method of predicting the effect that one metal can have upon another metal, when they are in electrical contact while being immersed in an electrolyte.

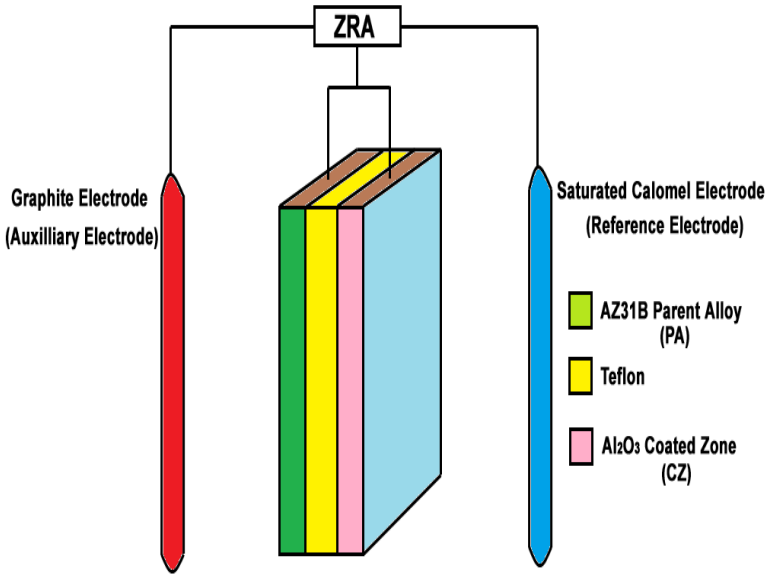

Fig. 1 Schematic diagram for the galvanic corrosion test

Fig. 1 shows the schematic diagram for the galvanic corrosion test. The galvanic test set up and samples were prepared as per ASTM G 82 (2004) [8]. A saturated calomel electrode and graphite electrode were used as the reference and auxiliary electrode respectively. The working electrodes were the HVOF sprayed titania coatings on AZ91D magnesium alloy, coupled with the AZ91D magnesium alloy base metal. An electrical contact was made between the galvanic couple, where a Teflon insulation of the same thickness as the HVOF sprayed titania coated AZ91D magnesium alloy and the base alloy is inserted, in-between the electrodes to avoid the direct contact between the electrodes. The couple electrodes were selected in two categories; identical electrodes couple from the coated zone, namely CZ/CZ, and identical electrodes from the base alloy PA/PA. Another couple electrodes set up was selected from two non-identical electrodes, one from the base alloy and the other from the coated zone, which is named as PA/ CZ. All the galvanic measurements were carried out at room temperature. The galvanic monitoring technique, also known as Zero Resistance Ammetry (ZRA) is another electrochemical measuring technique. With ZRA probes, two electrodes of dissimilar metals are exposed to the process fluid. When immersed in a solution, a natural voltage (potential) difference exists between the electrodes. The current generated due to this potential difference relates to the rate of corrosion, which is occurring on the more active of the electrode couple. If both the electrodes are identical then very little coupling current flows. In real life the two electrodes will be slightly different, one being more anodic or cathodic than the other, a small coupling current will exist.

The reason for choosing the identical couple electrodes is to compare the measured current density and corrosion potentials of these couples with those of the non-identical

couple electrodes, bearing in mind that theoretically there is no driving force for galvanic corrosion occurrence between two electrodes that are completely identical from the morphological and chemical composition points of view. The difference between two electrodes due to chemical composition or morphology can cause a galvanic cell formation, lead to the generation of current from the anode cell to the cathode cell.

The galvanic corrosion current density i_{corr}(A) for the AZ91D magnesium alloy and the galvanic corrosion current density i_{corr}(B) for HVOF sprayed titania coatings on AZ91D magnesium alloy are determined initially. When equal areas of the AZ91D Mg base metal and TiO_2 coatings were coupled, the resultant mixed potential of the system E_{corr}(AB) was at the intersection, where the total oxidation rate equals the total reduction rate. Initially, a test was conducted to predict the anode and cathode from the corrosion potentials individually. It was found that the HVOF sprayed titania coatings on AZ91D magnesium alloy couple (CZ/CZ) possess more negative potential than the parent alloy couple (PA/PA). The maximum difference between the corrosion potential of the identical couple electrodes was -70 mV. The average value of the corrosion potential for the CZ/CZ couple was -1240 mV, whilst for the PA/PA couple it was -1170 mV. The rate of oxidation of the individual coupled metals was such that the base metal corroded at a reduced rate i_{corr} (A), and the TiO_2 coated AZ91D magnesium alloy corroded at an increased rate i_{corr}(B). Hence, the TiO_2 coatings act as an anode, and the AZ91D base alloy acts as a cathode. Half cell reactions were carried out constituting a single cell. Thus, the current i_{corr}(AB) was the galvanic current which can be measured by Zero Resistance Ammetry (ZRA). The free corrosion potential of both the metals were found individually, and from the potential difference, the HVOF sprayed titania coated AZ91D

magnesium alloy was considered to be the anode, because of its more negative potential than the AZ91D base alloy, and the latter was the cathode.

2 Experimental Procedure

Commercial fused and crushed powders TiO_2 (99.9 wt. % purity), (Metalizing Equipment Company Pvt Ltd, Jodhpur, India) with appropriate particle size distributions for HVOF (-45 + 20 μm) spraying was used for coating preparation. A HVOF spray system was used to deposit the coatings. The main spray parameters are compiled in Table 1.

The electrochemical measurements were carried out using a flat three-electrode cell (Gill AC Potentiostat, ACM Instruments, England). In this test, an TiO_2 coated Mg sample was coupled to an uncoated Mg sample via a zero-resistance ammeter in a solution of NaCl. The galvanic couple was immersed in NaCl solution with different pH and chloride ion concentration for different immersion times of 1, 2.42, 4.5, 6.58 and 8 h.

Table 1 Optimized plasma spray parameters used to coat titania

Parameters	Unit	Values
Oxygen flow rate	lpm	253
LPG flow rate	lpm	63
Powder feed rate	gpm	34
Spray distance	mm	233
Carrier gas flow rate	lpm	12

Coating microstructure was investigated before and after the corrosion experiments by optical microscopy, SEM (Model: JEOL 6410-LV) and EDX analysis on metallographically polished cross sections and surfaces. The crystalline phase compositions of the coatings were analyzed by XRD analysis (Model: Rigaku ULTIMA-III). Fig.2 show the SEM morphologies of TiO_2 feedstock which shows the feedstocks

are angular and blocky and the X-ray diffraction analysis of feedstock reveals the anatase is the major phase and rutile is minor phase.

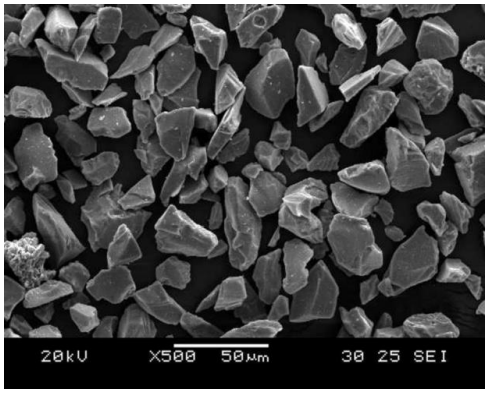

Fig. 2(a) SEM morphology of TiO_2 Powder

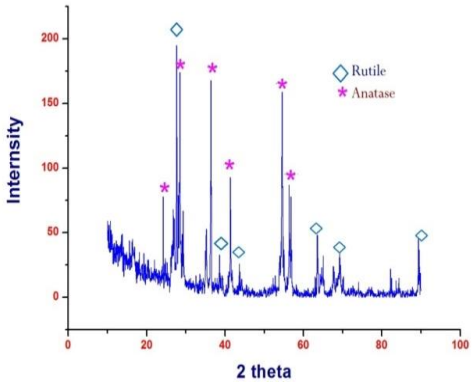

Fig. 2(b) XRD analysis

2.1 Finding the limits of corrosion test parameters

As the selection of corrosion process parameters, the feasible working limits of the parameters were taken for all uncoated and coated specimens. Table 2 presents the range of factors considered and Table 3 shows the 16 set of coded conditions used to form the design matrix.

Table 2 Important factors and their levels

S.No	Factor	Notation	Unit	Levels				
				-1.682	**-1**	**0**	**+1**	**+1.682**
1	pH value	*P*	-	3	4.82	7.5	10.18	12
2	Chloride ion concentration	*C*	Mole (M)	0.2	0.36	0.6	0.84	1
3	Exposure time	*T*	hours (h)	1	2.42	4.5	6.58	8

2.2 Developing empirical relationships

In the present investigation, to correlate the process parameters and the response, a second order quadratic model was developed to predict the response based on

experimentally measured values. The responses is a function of pH value (*P*), chloride ion concentration (*C*) and exposure time (*T*) and it could be expressed as,

Corrosion rate (CR) = f (*P*, *C*, *T*) ……. (1)

The empirical relationships include the main and interaction effects of all factors. The selected polynomial is expressed as follows

$Y = b_o + \Sigma b_i x_i + \Sigma b_{ii} x_i^2 + \Sigma b_{ij} x_i x_j$ ……(2)

For three factors, the selected polynomial can be expressed as

Table 3 Design matrix and experimental results

Expt No	Coded values			Original value			Corrosion rate (mm/yr)
	P	***C***	***T***	**pH**	**Cl^- (M)**	**Time (h)**	
1	-1	-1	-1	4.82	0.36	2.42	0.047
2	1	-1	-1	10.18	0.36	2.42	0.030
3	-1	1	-1	4.82	0.84	2.42	0.034
4	1	1	-1	10.18	0.84	2.42	0.011
5	-1	-1	1	4.82	0.36	6.58	0.058
6	1	-1	1	10.18	0.36	6.58	0.035
7	-1	1	1	4.82	0.84	6.58	0.052
8	1	1	1	10.18	0.84	6.58	0.032
9	-1.682	0	0	3	0.6	4.5	0.061
10	1.682	0	0	12	0.6	4.5	0.020
11	0	-1.682	0	7.5	0.2	4.5	0.018
12	0	1.682	0	7.5	1	4.5	0.053
13	0	0	-1.682	7.5	0.6	1	0.051
14	0	0	1.682	7.5	0.6	8	0.028
15	0	0	0	7.5	0.6	4.5	0.041
16	0	0	0	7.5	0.6	4.5	0.040
17	0	0	0	7.5	0.6	4.5	0.039

18	0	0	0	7.5	0.6	4.5	0.036
19	0	0	0	7.5	0.6	4.5	0.032
20	0	0	0	7.5	0.6	4.5	0.038

Corrosion Rate (CR) = b_0 +b_1 (P) + b_2 (C) +b_3 (T) + b_{11} (P^2) + b_{22} (C^2) + b_{33} (T^2) + b_{12} (PC) + b_{13} (PT) + b_{23} (CT) ……. (3)

To estimate the regression coefficients, a number of experimental design techniques are available. In this work, a three-factor five-level central composite rotatable design was used. The regression coefficients were calculated with the help of Design Expert V 8.0 statistical software. After determining the coefficients (at a 95% confidence level), the final empirical relationship was developed using these coefficients. The final statistical model to estimate the response is given below

Corrosion Rate = 0.055 - 7.31 x 10^{-3} * (*P*) + 0.015 * (*C*) + 2.74 x 10^{-3} * (*T*) + 4.25x10^{-3} *(*PC*) - 4.23 x 10^{-3} * (*PT*) + 4.5 x 10^{-3} *(*CT*) - 3.73 x 10^{-4}*(T^2) mm/yr…… (4)

2.3 Checking the adequacy of empirical relationship

In this investigation, analysis of variance (ANOVA) was used to check the adequacy of the developed empirical relationship. Test results of ANOVA of the response, namely, the corrosion rate, is presented in Table 4. The determination coefficient R^2 indicates the goodness of fit for the formulated empirical relationship. In all the considered cases, the value of the determination coefficient (R^2>0.99) indicates that, 1% of the total variations are not explained by the empirical relationship. The value of the adjusted determination coefficient is also high, which indicates the high significance of the empirical relationship. The predicted R^2 values also show good agreement with the adjusted R^2 values. The value of probability >F in Table 4 for the empirical relationship is <0.05, which indicates that the empirical relationship is significant. In this corrosion test *P, C, T,*

CT and C^2 are significant model terms. Lack of fit was not significant for all the developed empirical relationship, as it is desired [9]. The normal probability plot for the response corrosion rate is shown in Fig. 3. From the figure, it could be inferred that the residuals fall on the straight line, which shows that the errors are distributed normally [10]. Collectively, these results indicate the excellent capability of the regression model. Furthermore, each observed value matches its experimental value well, as shown in Fig. 4. The developed empirical relationship can be effectively used to predict the response by substituting the process parameter values in coded form.

Table 4 ANOVA test results for response

Source	*F* Value	*p*-value Prob > *F*
Model	27.66*****	< 0.0001
P	92.93*****	< 0.0001
C	117.12*****	< 0.0001
T	10.64*****	0.0085
PC	4.73	0.0547
PT	4.67	0.0559
CT	5.67*****	0.0385
P^2	2.82	0.1238
C^2	3.09	0.1091
T^2	6.51*****	0.0287
Lack of Fit	0.1808	
Std. Dev.	3.15×10^{-3}	
Mean	0.037	
R^2	0.9611	
Adj.R^2	0.9260	
Pred.R^2	0.7745	

*** Values of "Prob>*F*" less than 0.0500 indicate that the model terms are significant**

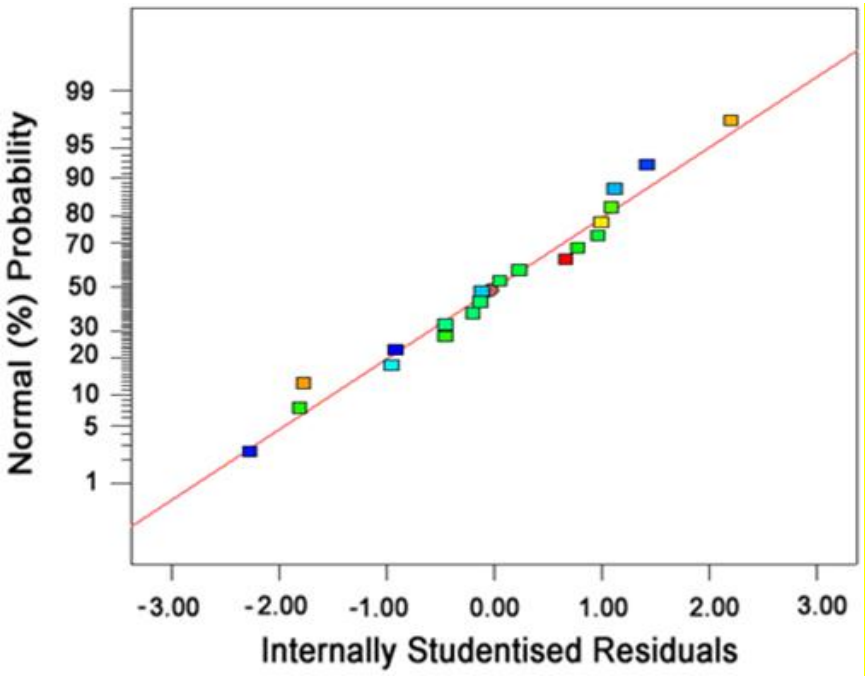

Fig.3 Normal probability plot for the response

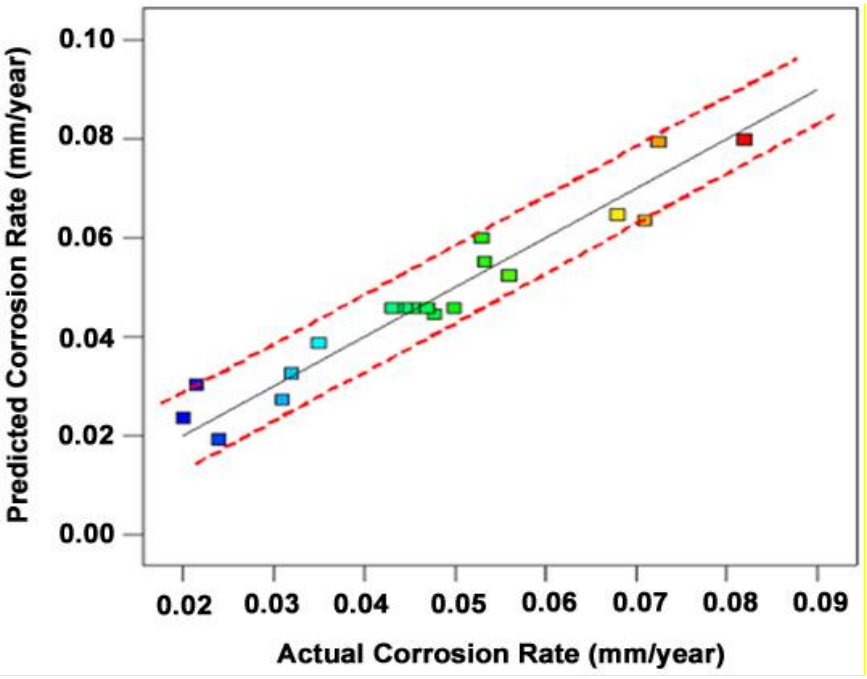

Fig.4 Correlation plot for the response

3 Results and Discussion

3.1 Effect of pH value on corrosion rate

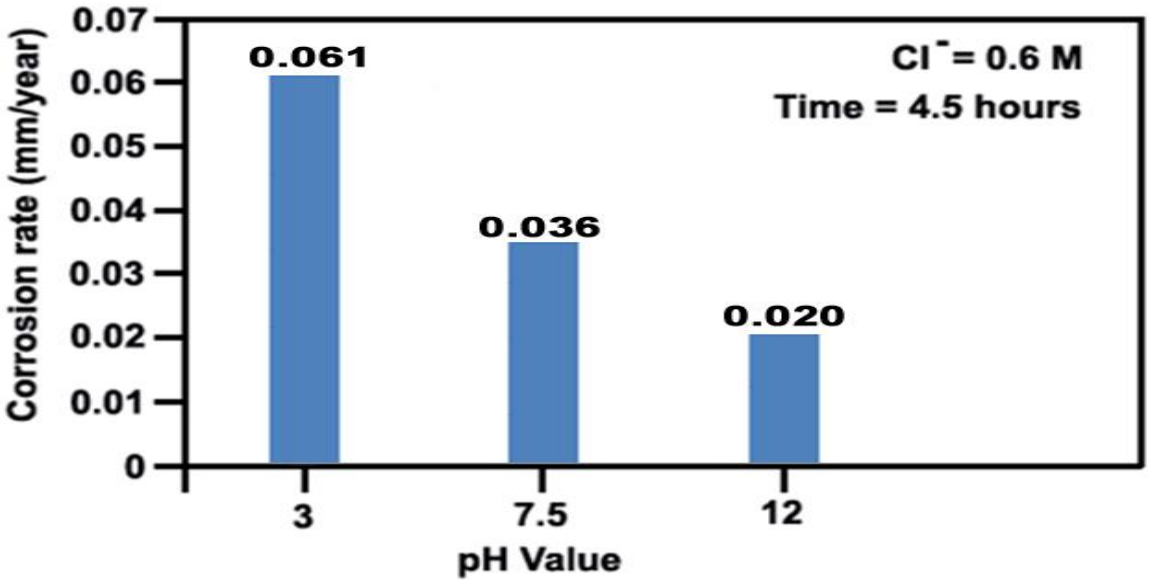

Fig. 5 Effect of pH on corrosion rate

The influence of the pH on the corrosion rate for during the galvanic corrosion test is presented in Fig. 5. It was found that, the galvanic current density decreases with the increase in the pH value. This means, that the anodic and cathodic activity between the magnesium base alloy and the HVOF sprayed titania coatings on AZ91D magnesium alloy decreases on increasing the pH value of the solution [11, 12]. In acidic solutions, the corrosion activity between the galvanic couple is enhanced, causing a higher galvanic current density, and this in turn, causes a higher corrosion rate.

The surface morphologies of scanned and SEM images of the uncoated and TiO_2-HVOF coatings after galvanic test are displayed in Figs.6 and 7. The corroded surface of native magnesium had a great amount of corrosion pits with big size and deep depth in some areas as an indication of intergranular corrosion shown in Fig. 7a. Beyond that, the structure of this layer has shown the characteristics of loose and porous, but the surface of coated sample still maintain uniform and a small amount of porous, there were only

slightly less corrosion pits formed (Fig. 7d). From the examination of the photographs of Fig. 7b it is obvious that the exposure of the uncoated coupons at the formation of voluminous corrosion products.

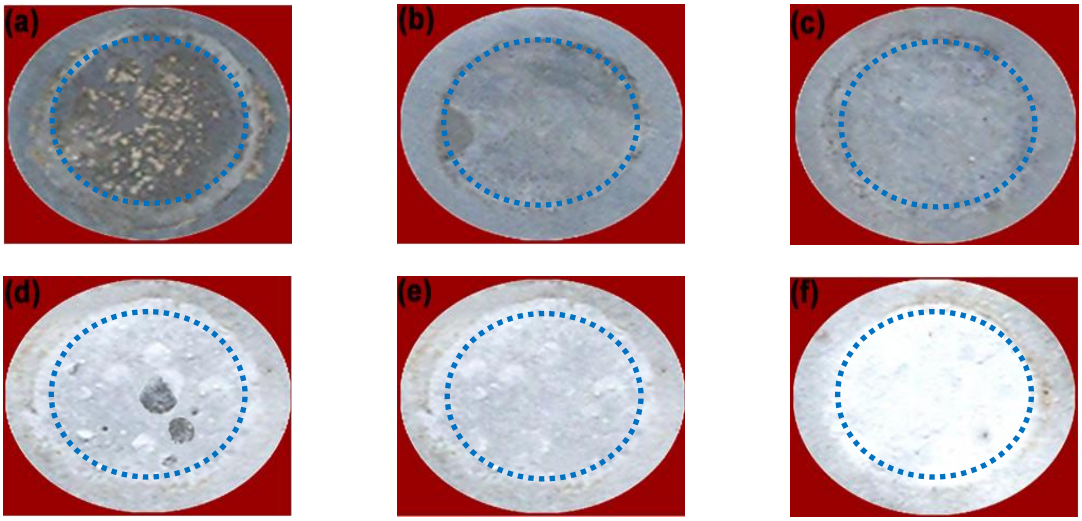

Fig. 6 Scanned images of the uncoated (a,b&c) and HVOF sprayed titania coated specimens (d,e&f) after galvanic corrosion test in NaCl solution

In comparison with the un-coated AZ91D, most areas on the coated samples are smooth without showing severe corrosion attack and there are only small amounts of corrosion products with a larger size which is schematically depicted in Fig.7e. Fig. 7c exhibits the typical morphology of the uncoated magnesium with localized corrosion. It is characterized by inhomogeneous white corrosion products and round corrosion pits. The coated sample surface is quite uniform and smooth and only small quantities of corrosion pits and white round particles are visible in the localized regions (Fig. 7f). The better corrosion resistance of the coated alloys may be attributed to the chemical stability of the ceramic oxide coating which acts as a barrier between the corrosion environment and substrate.

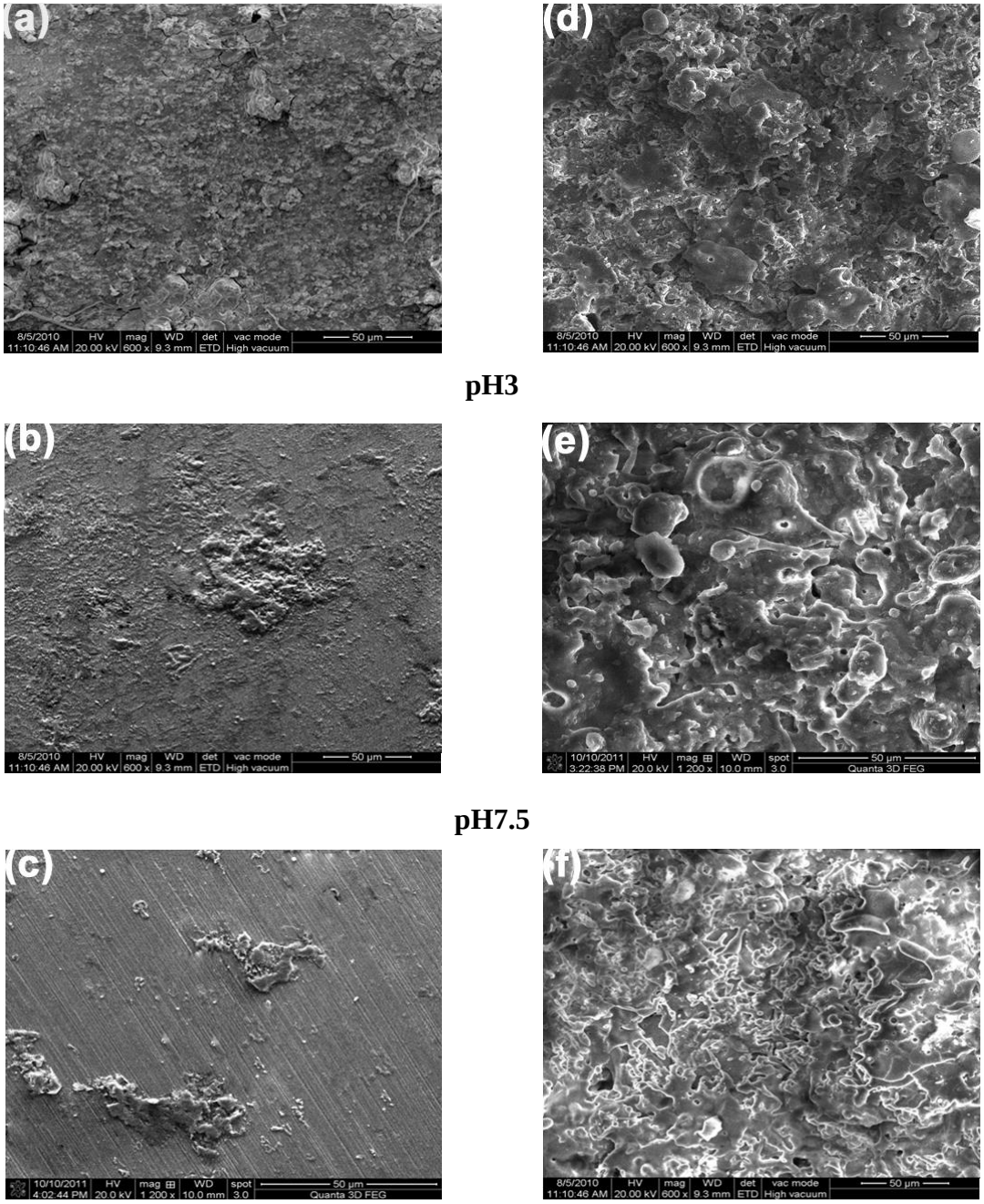

Fig.7 Effect of pH value on corrosion behavior of uncoated (a,b&c) and HVOF sprayed titania coated specimens (d,e&f) after galvanic corrosion test in NaCl solution

3.2 Effect of chloride ion concentration on corrosion rate

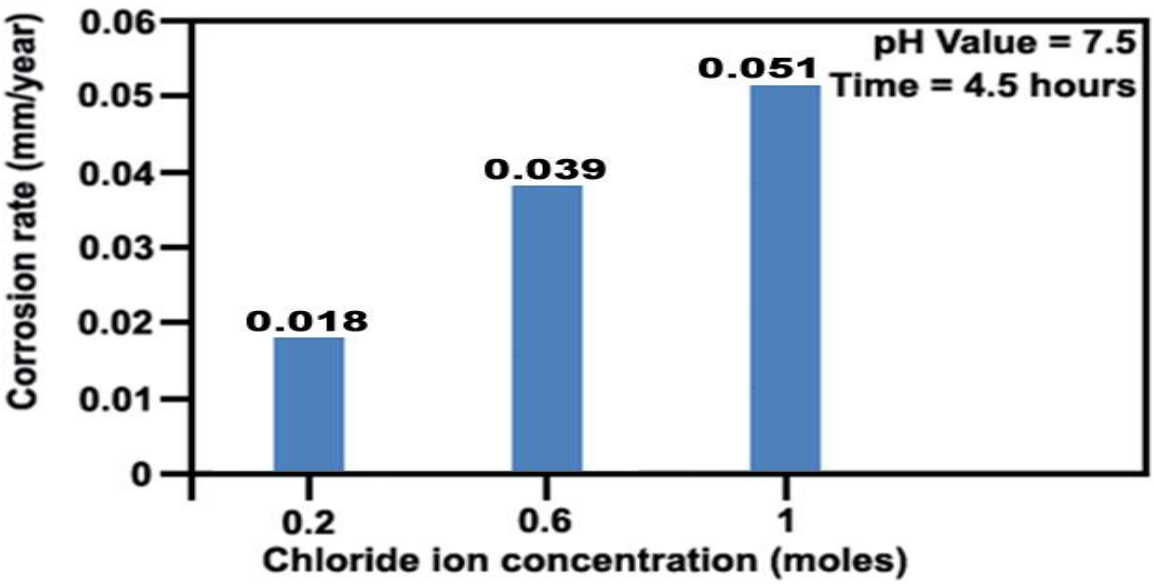

Fig. 8 Effect of chloride ion concentration on corrosion rate

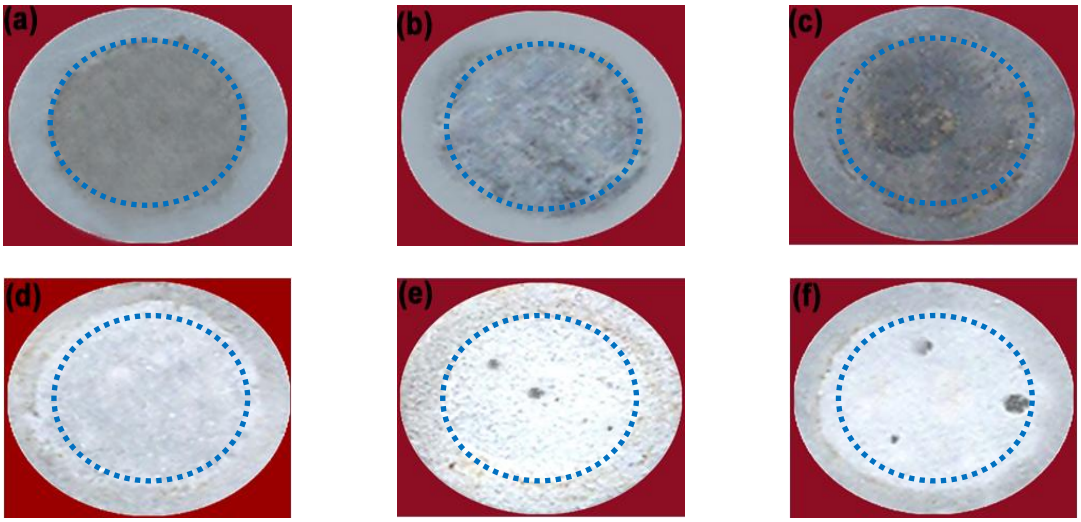

Cl^- 0.2M **Cl^- 0.6M** **Cl^- 1M**

Fig. 9 Scanned images of the uncoated (a,b&c) and HVOF sprayed titania coated specimens (d,e&f) after galvanic corrosion test in NaCl solution

Fig. 8 reveals the effect of the chloride ion concentration on the corrosion rate during the galvanic corrosion test. With the increase in the chloride ion concentration, the corrosion rate increases. The galvanic current density increases with the increase in the

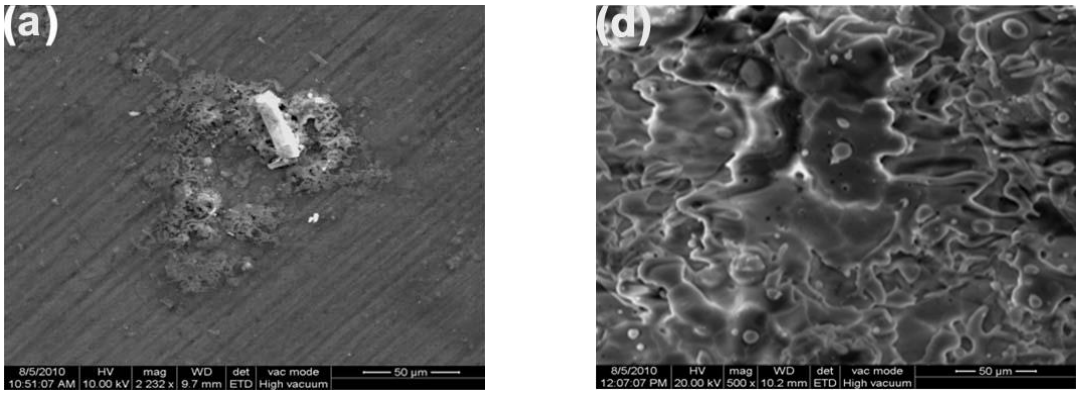

Cl^- 0.2M

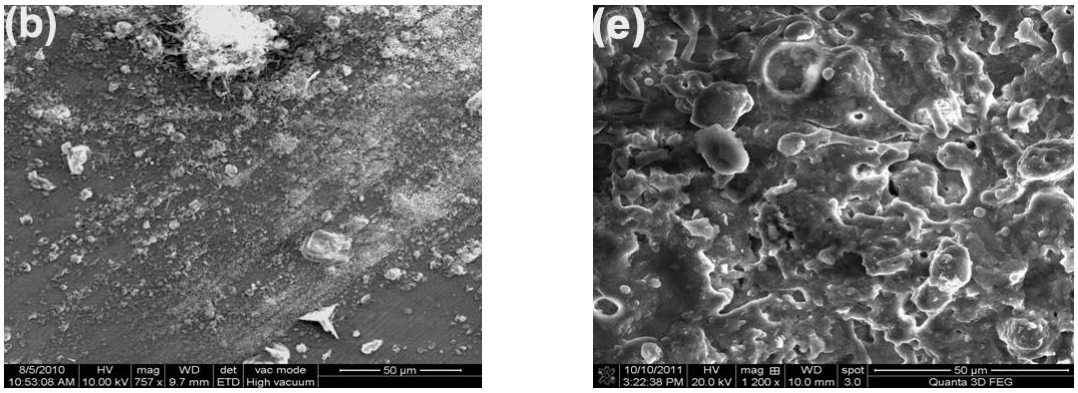

Cl^- 0.6M

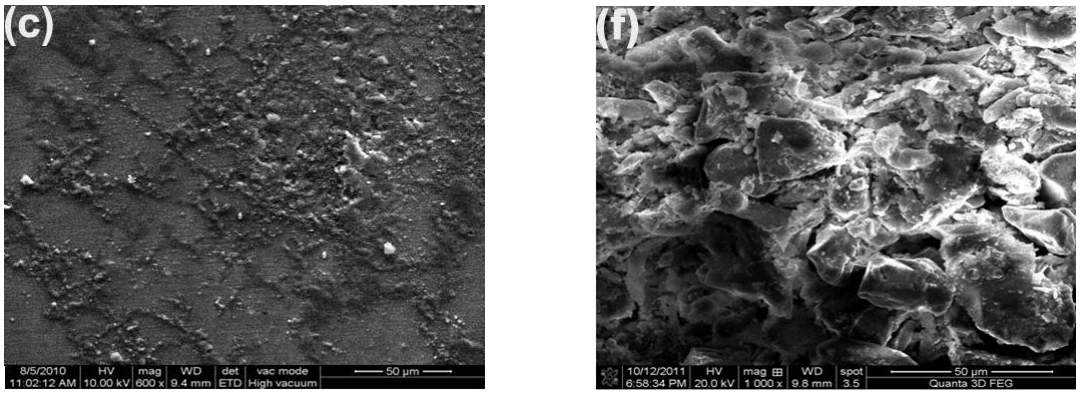

Cl^- 1M

Fig.10 Effect of chloride ion concentration on corrosion behavior of uncoated (a,b&c) and HVOF sprayed titania coated specimens (d,e&f) after galvanic corrosion test in NaCl solution

chloride ion concentration, causing the corrosion rate to be increased. It is observed that, the rising rate of corrosion was reduced during galvanic corrosion. This is due to the

formation of the metal-hydroxyl-chloride layer, which retards the migration of ions on the surface. It reduces the pace of the electrochemical corrosion rate to some extent [13, 14].

Figs. 9 and 10 illustrate the surface morphology of uncoated and TiO_2-HVOF coated Mg alloy after galvanic corrosion test. At lower chloride ion concentration no noticeable change was observed in the TiO_2-HVOF coating (Fig. 10d), but corrosion products were found on the surface of uncoated AZ31 Mg alloy (Fig. 10.9a). From the Fig.10.9e it can be clearly seen that the extent of corrosion damage is significantly reduced for HVOF sprayed titania coating as compared to uncoated AZ31 Mg alloy (Fig.10.9b). This result is consistent with the electrochemical results. The corroded surface of the TiO_2-HVOF coating in 1M NaCl solution reveals much smoother with few local corrosion pits occured on the sample (Fig. 10.9f). However, the SEM micrograph shown in Fig. 10.9c revealed localized corrosion damage was observed on the corroded surface. It was reported that the pitting of Mg occurs as a result of Cl^- adsorption and simultaneous Mg dissolution when Cl^- concentration exceeds 0.6M, and the needle-shaped corrosion products such as $MgCl_2$ or $Mg(OH)_2$ are formed around the pits. Thus, it is believed that the corrosion products were $Mg(OH)_2$ or $MgCl_2$ resulting from the pitting corrosion.

3.3 Effect of exposure time on corrosion rate

Fig.11 exhibits the effect of the exposure time on the corrosion rate for during the galvanic corrosion test. The galvanic current density decreases with the increasing exposure time. With the increase in exposure time, the anodic activity of the coating zone of the AZ91D magnesium alloy seems retarded, and the magnesium base alloy as a cathode dominates over it. Usually, the cathodic process liberates hydrogen, which tends to increase the concentration of OH^- ions, strengthening the surface from further corrosion. The rate of hydrogen evolution initially increased with increasing exposure

time. This is attributed to corrosion occurring over increasing fraction of the surface, which are the insoluble corrosion products.

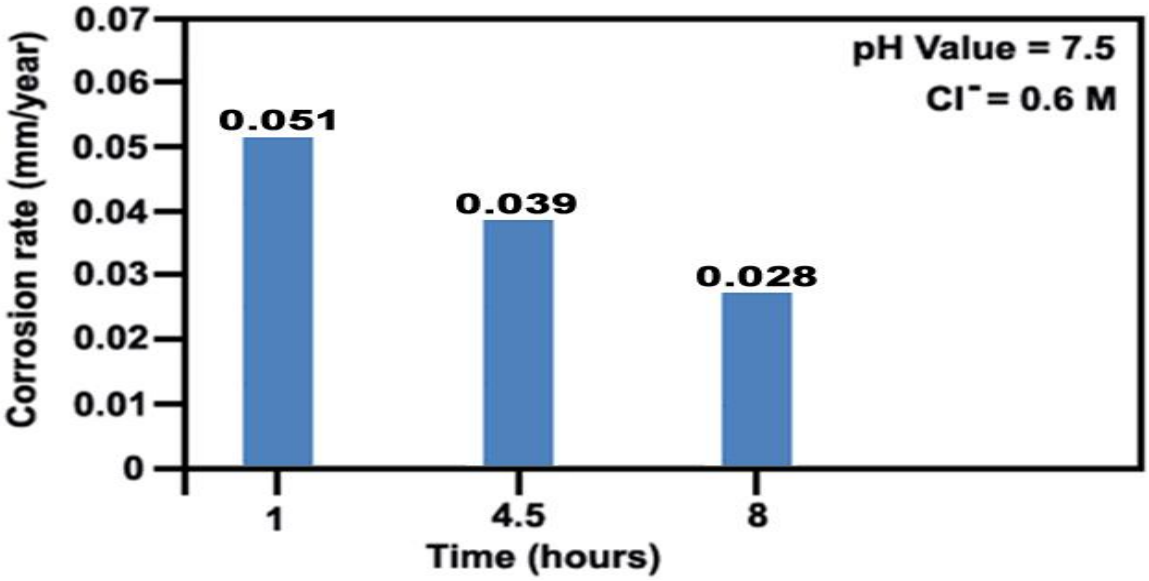

Fig.11Effect of exposure time on corrosion rate

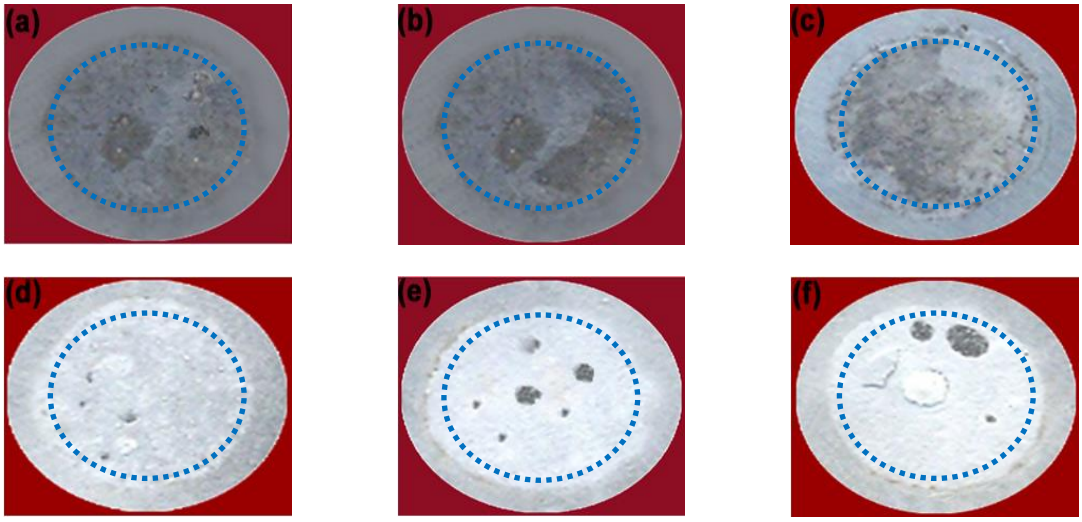

1h **4.5h** **8h**

Fig. 12 Scanned images of the uncoated (a,b&c) and HVOF sprayed titania coated specimens (d,e&f) after galvanic corrosion test in NaCl solution

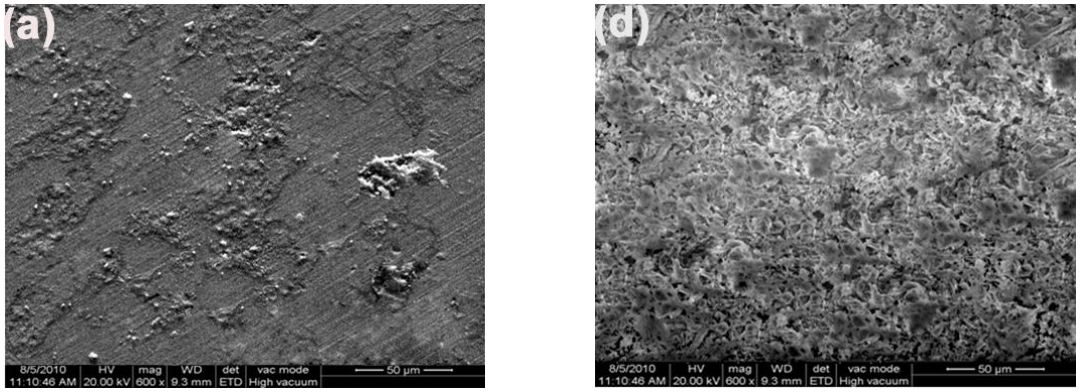

1h

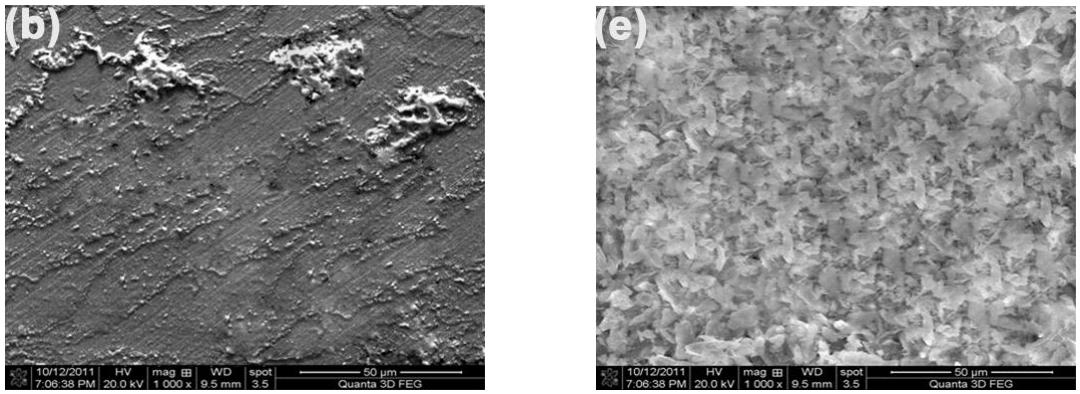

4.5h

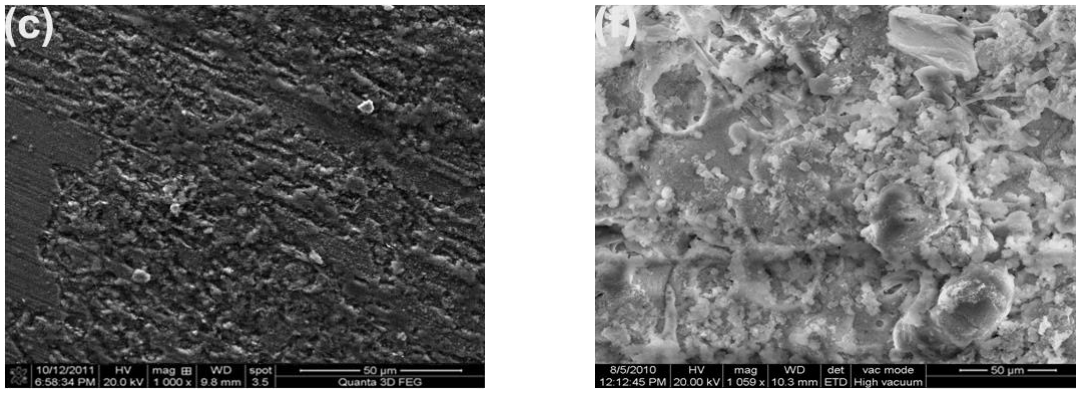

8h

Fig.13 Effect of exposure time on corrosion behavior of uncoated (a,b&c) and HVOF sprayed titania coated specimens (d,e&f) after galvanic corrosion test in NaCl solution

The SEM surface morphologies of uncoated and as-coated specimens are presented in Figs. 12 and 13 for comparison purposes. The surface of the coated substrate shows some clear and shallow corrosion stains (Fig.13d), while the uncoated sample shows severe corroded surface as shown in Fig.13a. Fig. 13b exhibits SEM morphology of the stacked corrosion products of the sample after immersed in NaCl solution for 4.5h. It is obvious that the corrosion products and thus provide nearly no protection against further corrosion. Referred to the literature [15], the main corrosion product is $Mg(OH)_2$. In the case of the TiO_2-HVOF coated specimen, slight dissolution had occurred at the pores on the corroded surface, as represented in Fig. 13e. When magnesium alloy was immersed in NaCl solution for 8 h as shown in Fig.13c, the filiform attacks got further aggravated. The surface was covered with a large number of corrosion filaments, resulting in that the tracks of corrosion filaments were difficult to be identified and the corrosion pits continued to grow in depth direction. With increasing the immersion time, the SEM micrograph shown in Fig.13f shows the higher amount of pores and cracks occurred on the corroded surface.

3.4 Corrosion products characteristics

Fig. 14 shows the XRD analysis to predict the composition of corrosion products and phase in the uncoated AZ91D specimen subjected to galvanic corrosion tests. All the characteristic peaks originate from the metallic Mg substrate and the β Phase. However, $Mg(OH)_2$ and MgO phases are detected in the specimen. Besides, many small peaks are present in the patterns from 10 to 30 degree, which could not be attributed to a single compound. They are mostly likely associated with $Mg_5(CO_3)_4(OH)_2.8H_2O$ considering that CO_2 naturally present. $Mg(OH)_2$ is the dominant product in the corrosion zone. $Mg(OH)_2$ (brucite) has a hexagonal crystal structure and undergoes easily basal cleavage causing cracking and curling in the film [17].

Fig. 15a and b displays the cross section and EDS analysis of as-sprayed titania coating on AZ91D magnesium alloy after 4.5 h of immersion in NaCl solution. The cross section images of as-sprayed coatings revealed significant signs of degradation in the coating/substrate interface. Fig. 15a evidences the extent of the corrosion

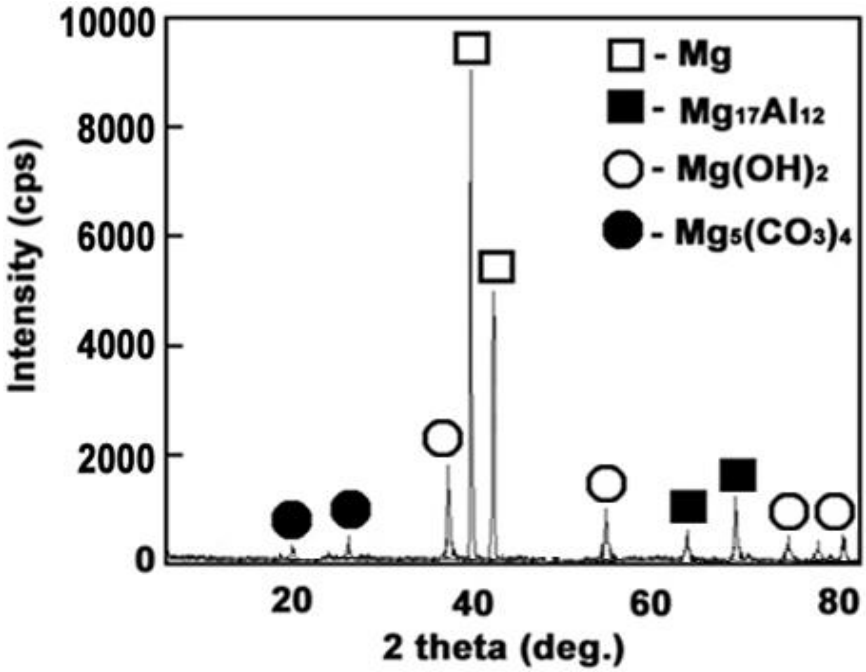

Fig. 14 XRD pattern for anodic specimen underwent galvanic corrosion

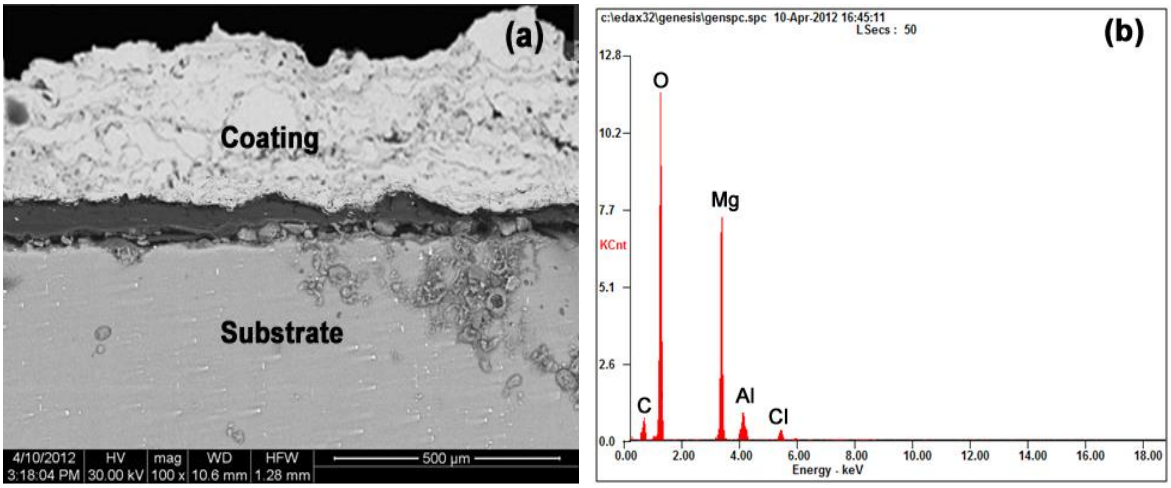

Fig. 15 (a) Cross section of as-sprayed titania coating on AZ91D magnesium alloy after 4.5 h of immersion in NaCl solution and (b) EDX analysis of coating–substrate interface.

process that occurs in the chloride medium, since the as-sprayed titania coating was detached from the AZ91D substrate after 4.5h of immersion. Examination of the coating/substrate interface showed the presence of corrosion products in this area, although only a part of them remained over the substrate or in the coating after the galvanic tests. According to EDX analysis (Fig. 15b), corrosion products rich in Mg and O were mainly detected in the interface area, along with a small amount of Al and of Cl.

4 Summary

The effects of corrosion test parameters such as pH value, chloride ion concentration and exposure time on the galvanic corrosion rate of the couple in NaCl solution have been analysed in detail. From the detailed analysis, the following conclusions have been drawn:

I. It is found that the galvanic couple exhibited an improved corrosion resistance with the increase in pH. The corrosion rate was higher at the acidic media than at the alkaline and neutral media with same concentrations and immersion time period.

II. It is also found that the galvanic couple corroded more seriously with the increase in Cl^- concentrations. More the Cl^- promoted the corrosion along with the rise in corrosion rate.

III. The investigation proved that, a corrosion resistivity with the increase of immersion time, resulting with the formation of hydroxide layer as a dominant factor to avoid the corrosion further.

Acknowledgements

The authors would like to acknowledge the Annamalai University for extending facilities to characterize the coatings. The authors also wish to thank Mr. R. SELVENDIRAN,

Technical Assistant, Department of Manufacturing Engineering, Annamalai University for his help in carrying out this investigation.

REFERENCES

1. *M. Sivapragash, P. Kumaradhas, B.S.J. Retnam, X.F. Joseph, and U.T.S. Pillai, Taguchi Based Genetic Approach for Optimizing the PVD Process Parameter for Coating ZrN on AZ91D Magnesium Alloy, Mater. Des., Vol. 90, pp. 713-722, (2006).*

2. *X. Lu, X. Feng, Y. Zuo, P. Zhang, and C. Zheng, Improvement of Protection Performance of Mg-Rich Epoxy Coating on AZ91D Magnesium Alloy by DC Anodic Oxidation, Prog. Org. Coat., Vol. 104, pp. 188-198, (2016).*

3. *D. Luo, Y. Liu, X. Yin, H. Wang, Z. Han, and L. Ren, Corrosion Inhibition of Hydrophobic Coatings Fabricated by Micro-Arc Oxidation on an Extruded Mg–5Sn–1Zn Alloy Substrate, J. Alloys Compd., Vol. 731(15), pp. 731-738, (2017).*

4. *M. Mohedano, C. Blawert, and M.L. Zheludkevich, Silicate- Based Plasma Electrolytic Oxidation (PEO) Coatings with Incorporated CeO2 Particles on AM50 Magnesium Alloy, Mater. Des., Vol. 86, pp. 735-744, (2015).*

5. *Y. Su, Y. Guo, Z. Huang, Z. Zhang, G. Li, J. Lian, and L. Ren, Preparation and Corrosion Behaviors of Calcium Phosphate Conversion Coating on Magnesium Alloy, Surf. Coat. Tech., Vol. 307, pp. 99-108, (2016).*

6. *S. Garcia-Rodriguez, A.J. Lopez, B. Torres, and J. Rams, 316L Stainless Steel Coatings on ZE41 Magnesium Alloy Using HVOF Thermal Spray for Corrosion Protection, Surf. Coat. Tech., Vol. 287, pp. 9-19, (2016).*

7. *ASTM G71-81, Standard Guide for Conducting and Evaluating Galvanic Corrosion Tests in Electrolytes, ASTM International, (2019).*

8. *ASTM G82-98, Standard Guide for Development and Use of a Galvanic Series for Predicting Galvanic Corrosion Performance, ASTM International, (2014).*

9. *A.S. Shahi and S. Pandey, Modelling of the effects of welding conditions on dilution of stainless steel claddings produced by gas metal arc welding procedures, J. Mater. Proc. Technol., Vol. 196, pp. 339-344, (2008).*

10. *S. Kumar, P. Kumar and H.S. Shan, Effect of evaporative pattern casting process. parameters on the surface roughness of Al-7% Si alloy castings, J. Mater. Proc. Technol., Vol. 182, pp. 615-623, (2007).*

11. *A. Atrens, G.L. Song, M.Z. LiuShi, F. Cao, M.S. Dargusch, Review of recent developments in the field of magnesium corrosion, Adv. Eng. Mater., Vol. 17, pp. 400-453, (2015).*

12. *H. Altun, S. Sen, Studies on the influence of chloride ion concentration and pH on the corrosion and electrochemical behaviour of AZ63 magnesium alloy, Mater Des., Vol. 25, pp. 637–43, (2004).*

13. *J. Liao, M. Hotta, Atmospheric corrosion behavior of field exposed magnesium alloys: Influences of chemical composition and microstructure, Corros. Sci., Vol. 100, pp. 353-364, (2015).*

14. *Q. Qu, S. Li, L. Li, L. Zuo, X. Ran, Y. Qu, B. Zhu, Adsorption and corrosion behaviour of Trichoderma harzianum for AZ31B magnesium alloy in artificial seawater, Corros. Sci., Vol. 118, pp. 12–23, (2017).*

15. *G. Song, A. Atrens, D. Stjohn, J. Nairn, Y. Li, The electrochemical corrosion of pure magnesium in 1 N NaCl, Corros. Sci., Vol. 39 (5), pp. 855–875, (1997).*

16. *G. Song, B. Johannesson, S. Hapugoda, D. Stjohn, Galvanic corrosion of magnesium alloy AZ91D in contact with an aluminium alloy, steel and zinc, Corros. Sci., Vol.46, pp. 955-977, (2004).*

17. *D. Huang, J. Hu, G.L. Song, X. Guo, Galvanic Corrosion and Inhibition of GW103 and AZ91D Mg Alloys Coupled to an Al Alloy in an Ethylene Glycol Solution at Ambient and Elevated Temperatures, Corros., Vol. 68, pp. 475–488, (2012).*